Scattering of electrons by atomic hydrogen at intermediate energies: Elastic scattering and $n=2$ excitation from 12 to 54 eV

Joseph Callaway
Department of Physics and Astronomy, Louisiana State University, Baton Rouge, Louisiana 70803-4001
(Received 13 March 1985)

Cross sections for elastic scattering and excitation of the $n=2$ states of atomic hydrogen by electrons are computed for incident energies in the range from 12 to 54 eV. The calculations are based primarily on an 11-state expansion including seven pseudostates. Pseudothresholds and pseudoresonances are suppressed by appropriate averaging.

I. INTRODUCTION

The scattering of electrons by hydrogen atoms is one of the most fundamental processes in atomic physics. In spite of a long history of studies reaching back for 50 years, progress has been slow, particularly in regard to the intermediate range of electron energies from the ionization threshold up to (loosely defined) energies at which high-energy approximations (Born, Glauber with variants and combinations) become valid. In a note published in 1983, McDowell and I found large uncertainties to exist even in the $n=2$ excitation cross sections, particularly in regard to the $2s$ state.[1]

This paper reports the results of calculations of elastic scattering and $n=2$ total excitation cross sections for incident electron energies from 12.2 ($k^2=0.90$ a.u.) to 54 eV. The calculations are of the close-coupling type, and employ a basis of 11 states including the exact $1s$, $2s$, $2p$, and $3d$ atomic states and seven pseudostates. (Details are given in Sec. II.) Results are determined on a rather fine grid of energies in this range so as to permit removal of pseudoresonance and pseudothreshold effects. In combination with results I have published previously for elastic scattering and $n=2$ excitation between the $n=2$ and $n=3$ thresholds,[2] a rather complete description of these processes is now available from the $n=2$ threshold up to four times the ionization energy. This will enable reliable calculations of rate coefficients or equivalent quantities for astrophysical and laboratory plasmas.

There is a vast literature concerning elastic scattering and $n=2$ excitation. Difficulties in interpreting the rather meager experimental data are summarized in Ref. 1. From the point of view of theory, the energy region of interest here is one of exceptional difficulty: The energies are too low for reliable application of high-energy approximations. But limited-basis close-coupling calculations also have serious problems, resulting from omission of continuum states of the target atom from the basis. Burke and Webb[3] were the first to introduce pseudostates in a close-coupling expansion for intermediate energies. Recent close-coupling calculations in this energy range have been described by Morgan[4] and Edmunds, McDowell, and Morgan.[5] These authors report cross sections (integrated, differential, and angular correlation parameters) at 35 and 54.4 eV. Several different close-coupling basis sets have been considered, but their calculations either do not include exchange, which is certainly not negligible at these energies, or use a local exchange potential.

I have previously reported results from pseudostate calculations (including exchange) at a limited number of energies.[6,7] However, uncertainties arose in those calculations from possible effects of pseudoresonances. Computational limitations caused inadequate convergence in variational calculations. In addition, it was not possible to make accurate computations for large values of the total angular momentum. As a result, differential cross sections and angular correlation parameters were not accurate, particularly at 54.4 eV, and for large scattering angles.

In the work reported here, I have attempted to eliminate pseudoresonance and pseudothreshold effects by means of the amplitude-fitting technique introduced by Burke *et al.*[8] This procedure will be discussed in detail in Sec. II. Calculations have been made for a large number of values of the incident energy (106 for the S, P, and D partial waves and a smaller number for higher L). The results, presented in Sec. III, give a very detailed picture of the energy dependence of the elastic and excitation cross sections. Some improvements have been made in the variational programs to enable calculations for larger L than heretofore, but the results will be adequate for the description of angle-dependent properties only in the lower-energy portion of the range considered. The effective collision strength (a thermal average) is discussed in Sec. IV.

II. METHOD

In this section we will consider specifically some particular features of our calculational procedures which have not been extensively discussed previously. A comprehensive discussion of the principles and practices of variational calculations is given in Ref. 6. In general, improvements in the calculational facilities available have made possible substantial improvements in numerical accuracy. This has been accomplished quite straightforwardly by increasing the size of the basis of short-range functions used in the calculation of the scattering wave function to about 25 Slater-type orbitals (STO's) per channel and by using

quadruple precision for certain critical parts of the calculations. Energy-dependent basis functions of the form $(1-e^{-\gamma r})^j \sin(kr)/r^n$ and $(1-e^{-\gamma r})^j \cos(kr)/r^n$ are also included, for $n=2$, 3 and k, the wave vector for open channels other than that associated with the atomic $1s$ state.

The points I wish to discuss is more detail concern (i) the problem of removing structure associated with pseudostate thresholds from the calculated amplitudes, and (ii) the changes that have been made in our calculational procedures to enable results to be obtained for larger values of the total angular momentum L.

A. Pseudostates

The present calculation employs an expansion of the wave function for the two-particle system in a basis of eleven states, including four exact states ($1s$, $2s$, $2p$, and $3d$) and seven pseudostates. There are in all 5 s states, 4 p states, and 2 d states in the basis. The basis is that labeled "standard 5-4-2" in Ref. 6. Two other sets of the same size have been considered for comparison purposes. The radial wave function of the states can be expressed as

$$R_j^{(l)}(r)=\sum_i c_{ji}^{(l)} r^{n_i} e^{-\zeta_i r} \tag{2.1}$$

in which j is the state number and l is the angular momentum. The parameters and energies of the state in all the sets are listed in Table I. The discussion below refers to the standard 5-4-2 set. It will be observed that one of the s states has an energy which is a reasonable approximation to that of the actual $3s$ state, and similarly one of the p states approximates the $3p$; the other pseudostates have energies in the continuum. Three of the pseudostates have energies quite close to the ionization threshold.

In the range of energies from $k^2=0.90$ a.u. to $k^2=4.0$ a.u., there are five pseudothresholds, one of p symmetry at $k^2=2.24$ a.u., another of s symmetry at $k^2=2.70$ a.u. plus three; one each of s, p, and d symmetry close to $k^2=1.0$ a.u. Structure associated with these pseudothresholds was found in all the partial waves considered with the exception of ^3S. This structure was removed by the amplitude- (or T-matrix) fitting technique introduced in Ref. 8.

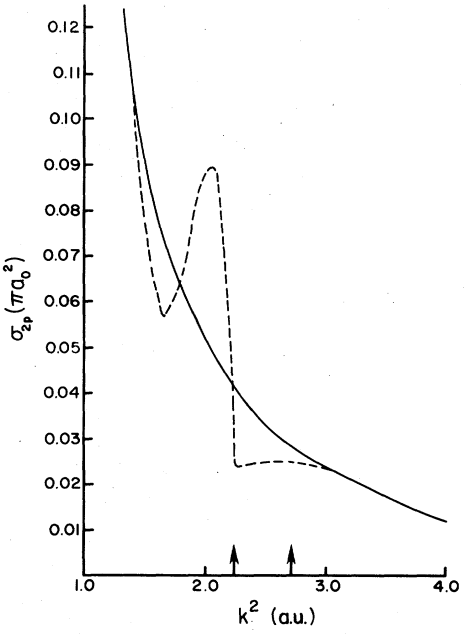

FIG. 1. Effect of pseudothreshold structure on the ^1D partial cross section for $2p$ excitation. Arrows indicate the position of the two pseudothresholds. The smooth solid curve shows the result of amplitude fitting as described in the text.

An example of the structure found is shown in Fig. 1, which shows a portion of the ^1D partial cross section for the $1s \rightarrow 2p$ transition. It is seen that the most prominent structure is that associated with the 2.24-Ry threshold,

TABLE I. Parameters of the pseudostate sets used in this work [refer to Eq. (2.1)]. The energies of the pseudostates are also given. Note that the energies refer to the states rather than to the individual orbitals. Most calculations employ the standard 5-4-2 set.

	Standard 5-4-2 basic set			Variant 5-4-2 basic set			VTPS		
	n_i	ζ_i	E_j	n_i	ζ_i	E_j	n_i	ζ_i	E_j
$l=0$									
$i=1$	0	1.0	−1.0	0	1.0	−1.0	0	1.0	−1.0
$i=2$	0	0.5	−0.25	0	0.5	−0.25	0	0.5	−0.25
$i=3$	1	0.5	−0.1093	1	0.5	−0.1093	1	0.5	−0.0523
$i=4$	0	0.8	0.0307	0	0.8	0.0307	1	1.0	0.6810
$i=5$	1	0.2	1.7073	1	0.2	1.7073	0	1.5	6.2674
$l=1$									
$i=1$	1	1.0	−0.25	1	1.0	−0.25	1	1.0	−0.25
$i=2$	1	0.8	−0.1090	1	0.5	−0.1094	1	0.5	−0.0709
$i=3$	1	0.5	0.0352	1	0.2	−0.0239	2	1.0	0.3803
$i=4$	1	0.2	1.2413	2	0.5	0.8179	1	0.8	2.6023
$l=2$									
$i=1$	2	0.5	−0.1111	2	0.8	−0.1111	2	1.0	0.0397
$i=2$	2	$\frac{1}{3}$	0.00065	2	$\frac{1}{3}$	0.1882	3	1.0	1.1983

while the 2.70-Ry threshold is hardly noticeable. The broad scale and large amplitude of the structure should be noticed. The ^1D partial wave is a major contributor to $2p$ excitation; and the structure would produce noticeable irregularities in the total cross section.

Previous experience with pseudoresonances suggests that if it were practical to include several more pseudostates in the basis, the structure associated with the pseudothresholds would become narrower, and diminish in amplitude.[9,10] However, with a basis set of limited size, we are forced to attempt to remove this structure, and extract a smooth background part. There are two ways in which this can be done: It may be possible to locate a specific pole (or poles) in K matrix and set the residue equal to zero.[11] This process seems to work well in some cases of electron-ion scattering in which pseudothreshold structure other than a resonance is unimportant. However, this procedure does not seem to be satisfactory in the electron-hydrogen problem because we observe in some partial waves (^1S, for example) pseudothreshold structure without (apparently) any indication of K-matrix poles. Further there are five pseudothresholds in the present problem, three of which are relatively close together. In the illustration of Fig. 1, there is a major resonance below the $k^2=2.24$ threshold, but the cross section does not resume its generally decreasing trend until after the higher threshold is passed. An alternative procedure is amplitude fitting, as recommended by Burke *et al.*[8]

In this method, which is employed here, least-squares fits are made to the scattering and transition amplitudes using low-order polynomials in the energy. If f_{ij} is the amplitude for the transition $i\rightarrow j$ for fixed values of the channel quantum numbers L, S, etc. (which are suppressed), we have

$$f_{ij}=\sum_{k=0}^{K} a_{ij}^{(k)}E^k \tag{2.2}$$

in which the coefficients $a_{ij}^{(k)}$ are complex. If the expression is restricted to relatively small powers of the energy, the rapid variation of the amplitudes at pseudoresonances and pseudothresholds will not be reproduced. The unphysical structure will be removed. In these calculations, I have usually set $K=6$: a polynomial of sixth order seems to be needed adequately to represent the general trend of the data over the large energy range considered. Tests in a model problem have shown that this procedure enables the extraction of elastic and excitation cross sections within a few percent of the exact results.[9,10] The effect of amplitude averaging on the $2p$ excitation cross section in the ^1D partial wave is shown in Fig. 1. A smooth interpolation is achieved throughout the region of pseudothreshold phenomena.

B. Higher angular momenta

In this, as in my previous work,[2,6] the coupled integro-differential equations which result when the pseudostate expansion is substituted into the Schrödinger equation are solved by variational methods. A major limitation of these calculations is that they become increasingly cumbersome and time consuming as the angular momentum increases. There have also been accuracy problems for large L.

One of the major sources of difficulty for large L has been the proper choice of the irregular asymptotic function. It will be recalled that in the variational approach, we require two independent functions in each channel, S_l and C_l, such that for large r

$$\begin{aligned} rS_l &\sim \sin(kr-l\pi/2)\ , \\ rC_l &\sim \cos(kr-l\pi/2)\ , \end{aligned} \tag{2.3}$$

but for small r, both S_l and C_l must be regular, i.e., proportional to r^l. A very satisfactory choice for S_l is just $k^{1/2}j_l(kr)$; the problem is C_l. Armstead proposed[12] to use a combination of j_{l+1} and j_{l+2}: $k^{1/2}[j_{l+1}(kr)+(l+1)/krj_{l+2}(kr)]$, and this choice has been followed by Lyons and Nesbet.[13] This combination has the property that the two leading terms in $1/r$ in the large-r form agree with the corresponding terms in the irregular Bessel function n_l. My experience is that this choice is not optimum for large l and small-channel wave vector k, because the function is then close to zero over a large range of values of r, and assumes the asymptotic form only very far from the nucleus, e.g., much further than j_l itself. I examined the choice $(1-e^{-\beta r})^{2l+1}n_l(kr)$, where the factor multiplying n_l gives regular behavior near the origin, but found an undesirable degree of sensitivity to the parameter β and an undesirable tendency for the function to peak at small r if β were not chosen very carefully. So I returned as far as the irregular function is concerned, to the truncated irregular Bessel function discussed in Ref. 5, which is for $l>0$,

$$C_l=(1-e^{-\beta r})^{l+2}\bar{n}_l(kr) \tag{2.4}$$

where $\bar{n}_l$ contains only the leading $(1/r)$ and $(1/r)^2$ terms in the full irregular function. This choice of irregular function, in combination with the use of the complete regular function $j_l(kr)$ [in Ref. 6, a truncated form of j_l was also employed], is the most satisfactory choice of asymptotic functions I have tested. The value of β is an arbitrary parameter subject to variation: $\beta=1.2$ works well for small L, but needs to be smaller (0.6 or 0.8) for $L=4$ or 5.

It is characteristic of the variational method that a very high degree of accuracy must be maintained in evaluation of the so called bound-free integrals (see Ref. 6)—which are far more critical to the success of the calculation than the apparently more complicated free-free integrals. The choices advocated above make possible analytic evaluation of these integrals, but also raises the problem that in order to maintain sufficient accuracy in the process, it is necessary to employ quadruple-precision [128-bit (binary digit)] arithmetic. This is about a factor of 10 slower than double-precision (64-bit) arithmetic on an IBM 3081 and has caused the present calculations to be restricted to $L\lesssim 5$. A smaller pseudostate basis of 3 s and 3 p functions (exact $1s$, $2s$, and $2p$ states plus three pseudostates) was used for $L=4$ and 5.

The integrated cross section for elastic scattering is well converged throughout the energy range considered when

the calculations are limited to $L \leq 5$. This is not true for the differential cross section, where the contributions of a large number of partial waves is significant particularly for large scattering angles.

The integrated cross section of $2s$ excitation is also reasonably well converged when the calculations are limited to $L \leq 5$. At $k^2=1.10$, I estimate that only 0.6% of the $2s$-cross-section results from partial waves of $l \geq 6$; while at $k^2=4.0$, the estimated amount is 26%. In contrast, only in the low-energy portion of the energy range is the $2p$ cross section well converged in L at $L=5$. At $k^2=1.1$, I estimate that 2.1% of this cross section derives from $L \leq 6$. At $k^2=2.75$, half of the total cross section derives from $L \geq 6$, and at $k^2=4.0$, the proportion is 68%.

Consequently, some method of estimating the high-L contribution is essential. In this paper, the unitarized Born approximation with exchange (UBX) has been employed. The accuracy of this approximation is probably not very great, but it should be at its best for $2p$ excitation. A contribution from this source has been included for all the transitions studied here.

III. RESULTS AND DISCUSSION

The calculations proceeded as follows: In the S, P, and D partial waves, 11-state calculations of scattering and transition amplitudes were made on a grid of energies separated by approximately 0.01 Ry from $k^2=0.90$ to 1.10, by approximately 0.03 Ry from $k^2=1.10$ to 3.0, and at intervals of 0.05 Ry from $k^2=3.0$ to 4.0. Somewhat larger spacings were used for $L=3$, 4, and 5. In the latter two cases ($L=4,5$), as mentioned previously, a smaller 3 s—3 p basis was used (which contained the exact $1s$, $2s$, and $2p$ functions plus 1 s-type and 2 p-type pseudostates). The amplitudes were stored and the amplitude fitting procedure, as discussed previously, was applied. For $L=3$, 4, and 5 the amplitude fits were used to generate partial

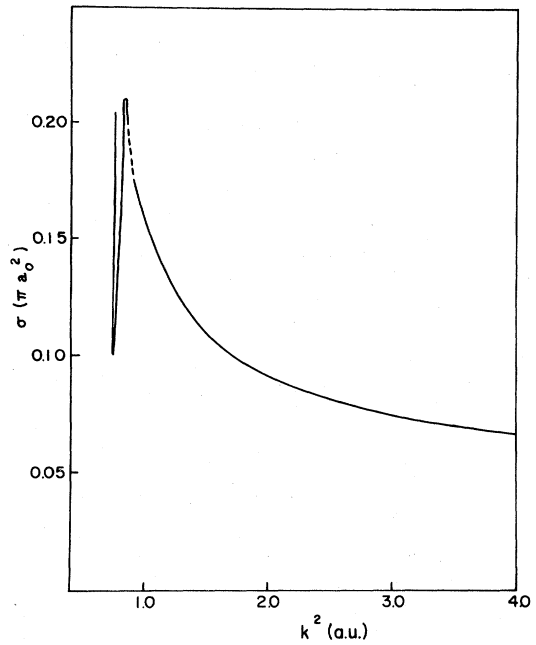

FIG. 3. Cross section for $2s$ excitation (units πa_0^2) from $k^2=0.75$ to 4.0. The vertical line near $k^2=0.75$ represents the shape resonance close to threshold. Resonances close to the $n=3$ threshold are not shown. A dashed line indicates the resonance region.

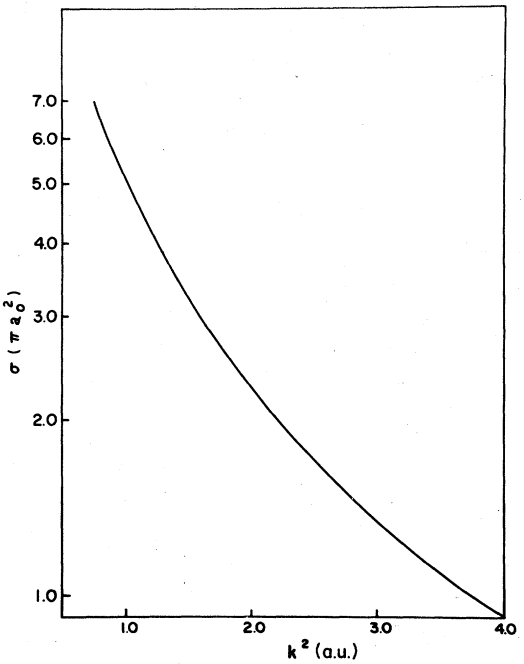

FIG. 2. Elastic cross section (units πa_0^2) from $k^2=0.75$ to 4.0.

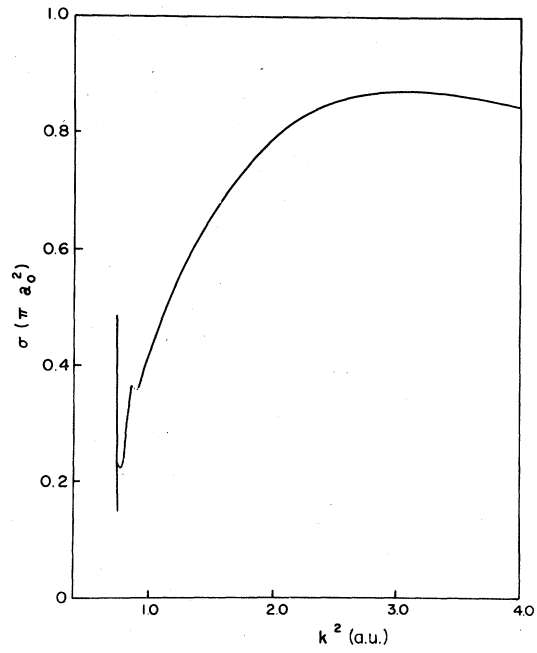

FIG. 4. Cross section for $2p$ excitation (units πa_0^2) from $k^2=0.75$ to 4.0. Lines are as in Fig. 3.

TABLE II. Calculated cross sections (πa_0^2) as functions of k^2 (a.u.).

k^2	σ_{1s}	σ_{2s}	σ_{2p}	k^2	σ_{1s}	σ_{2s}	σ_{2p}
0.90	5.815	0.174	0.357	2.05	2.208	0.091	0.806
0.91	5.749	0.170	0.357	2.08	2.167	0.091	0.811
0.92	5.681	0.168	0.361	2.11	2.128	0.090	0.816
0.93	5.616	0.165	0.373	2.14	2.090	0.089	0.821
0.94	5.544	0.163	0.389	2.17	2.053	0.089	0.825
0.95	5.478	0.161	0.392	2.20	2.018	0.088	0.829
0.96	5.421	0.159	0.397	2.23	1.983	0.087	0.833
0.97	5.364	0.157	0.402	2.25	1.960	0.087	0.836
0.98	5.308	0.156	0.406	2.28	1.927	0.087	0.839
0.99	5.252	0.154	0.412	2.31	1.895	0.086	0.842
1.00	5.198	0.154	0.417	2.34	1.864	0.085	0.845
1.01	5.148	0.152	0.422	2.37	1.834	0.085	0.848
1.02	5.096	0.151	0.427	2.40	1.804	0.084	0.851
1.03	5.044	0.150	0.432	2.43	1.775	0.083	0.853
1.04	4.983	0.149	0.437	2.46	1.747	0.083	0.855
1.05	4.936	0.148	0.442	2.49	1.720	0.082	0.857
1.06	4.886	0.147	0.448	2.52	1.694	0.081	0.859
1.07	4.837	0.147	0.455	2.55	1.668	0.081	0.861
1.08	4.778	0.146	0.461	2.58	1.643	0.080	0.862
1.09	4.740	0.145	0.467	2.61	1.618	0.080	0.864
1.10	4.694	0.145	0.472	2.64	1.594	0.079	0.865
1.11	4.647	0.144	0.477	2.67	1.570	0.079	0.866
1.13	4.556	0.142	0.486	2.70	1.548	0.078	0.867
1.15	4.467	0.140	0.497	2.73	1.526	0.078	0.868
1.18	4.339	0.138	0.511	2.75	1.511	0.077	0.869
1.21	4.216	0.135	0.525	2.79	1.483	0.077	0.869
1.24	4.098	0.132	0.539	2.82	1.462	0.076	0.870
1.27	3.986	0.129	0.553	2.85	1.442	0.076	0.871
1.30	3.878	0.126	0.566	2.88	1.422	0.076	0.871
1.33	3.738	0.123	0.580	2.91	1.403	0.075	0.872
1.36	3.674	0.119	0.592	2.94	1.384	0.075	0.872
1.39	3.579	0.116	0.605	2.97	1.366	0.075	0.873
1.42	3.487	0.113	0.617	3.00	1.348	0.075	0.873
1.44	3.429	0.111	0.626	3.05	1.318	0.074	0.873
1.47	3.343	0.109	0.637	3.10	1.290	0.074	0.873
1.50	3.261	0.107	0.649	3.15	1.263	0.074	0.872
1.53	3.182	0.106	0.661	3.20	1.237	0.074	0.872
1.56	3.108	0.104	0.671	3.25	1.212	0.074	0.872
1.59	3.037	0.103	0.682	3.30	1.187	0.074	0.871
1.62	2.968	0.101	0.693	3.35	1.164	0.074	0.870
1.65	2.903	0.100	0.703	3.40	1.141	0.073	0.869
1.69	2.812	0.099	0.716	3.45	1.118	0.073	0.868
1.73	2.732	0.098	0.729	3.50	1.097	0.073	0.866
1.76	2.674	0.097	0.738	3.55	1.076	0.073	0.865
1.79	2.619	0.096	0.747	3.60	1.056	0.072	0.864
1.82	2.565	0.096	0.755	3.65	1.037	0.072	0.862
1.85	2.513	0.095	0.763	3.70	1.018	0.071	0.860
1.88	2.463	0.094	0.770	3.75	1.000	0.071	0.858
1.91	2.414	0.094	0.777	3.80	0.982	0.070	0.856
1.94	2.367	0.093	0.784	3.85	0.965	0.069	0.854
1.96	2.337	0.093	0.789	3.90	0.950	0.068	0.853
1.99	2.292	0.092	0.795	3.95	0.934	0.067	0.851
2.02	2.249	0.092	0.800	4.00	0.920	0.066	0.849

cross sections at the same energies as used for $L=0$, 1, and 2. The cross sections resulting from this process were combined. The unitarized Born approximation was used estimate contributions from partial waves with $L \geq 6$.

The calculated cross sections for elastic scattering and for excitation of the $n=2$ states are given numerically in Table II, and are shown graphically in Figs. 2–4. These figures include the region between the $n=2$ and $n=3$ thresholds as obtained in Ref. 2, but do not show the detailed structure of Feshbach resonances under the $n=3$

TABLE III. Elastic scattering amplitudes at selected energies.

	1.10		1.21		1.44		2.25		4.00	
k^2	R	I	R	I	R	I	R	I	R	I
^1S	0.396	0.476	0.372	0.452	0.362	0.444	0.331	0.411	0.337	0.365
^3S	0.191	0.959	0.231	0.939	0.297	0.893	0.415	0.749	0.474	0.559
^1P	0.032	0.041	0.035	0.054	0.048	0.065	0.088	0.095	0.129	0.105
^3P	0.377	0.188	0.375	0.186	0.371	0.181	0.350	0.163	0.316	0.135
^1D	0.088	0.066	0.079	0.080	0.076	0.077	0.064	0.096	0.061	0.079
^3D	0.101	0.014	0.106	0.017	0.116	0.022	0.129	0.034	0.142	0.040
^1F	0.047	0.011	0.051	0.017	0.056	0.024	0.052	0.050	0.047	0.054
^3F	0.044	0.010	0.045	0.012	0.051	0.017	0.054	0.023	0.067	0.027
^1G	0.022	0.003	0.025	0.005	0.029	0.010	0.031	0.025	0.026	0.033
^3G	0.022	0.003	0.024	0.004	0.028	0.009	0.031	0.017	0.036	0.022
^1H	0.012	0.001	0.013	0.002	0.016	0.004	0.020	0.010	0.019	0.022
^3H	0.012	0.001	0.013	0.002	0.016	0.003	0.021	0.011	0.022	0.017

threshold, which are too narrow and too irregular to be represented on these graphs. That region is shown in detail in Ref. 2. Elastic scattering and transition amplitudes are listed at five selected energies in Tables III—V. These supersede tables of this type that I have published previously. The amplitudes for $k^2=1.10$ and 2.25 are those obtained from the amplitude-fitting procedure, while for $k^2=1.21$, 1.44, and 4.0, I have given unmodified amplitudes.

The elastic scattering cross section is a steadily decreasing function of energy. For $k^2>3.0$, it exhibits a good approximation to $1/k^2$ behavior, but the magnitude of the cross section is, in this range of energies, always substantially larger than the high-energy Born (or Glauber) results ($\sigma_{FB}=\sigma_G=7/3k^2$ in the units used here). Throughout the entire range two partial waves, ^3S and ^3P dominate the elastic scattering. The ^3S partial cross sections depend only very weakly on the pseudostate basis employed and do not show any obvious pseudoresonance structure. There is a small contribution from high partial waves, but this should be accurately determinable from the polarizability. The principal errors in the elastic scattering probably come from the failure of the basis set to describe short-range correlations adequately, but this affects principally the ^1S partial wave. These considerations suggest that the present elastic cross section may be correct within 3—5%. The present results agree within about 3% with a nine-state R-matrix calculation of Fon *et al.*[14]

The $2s$ excitation cross section is strongly affected by the introduction of pseudostates. The values obtained in these calculations are about a factor of 2.4 below those obtained in three state close-coupling computations at $k^2=1.44$ (19.6 eV).[15] Figure 3 shows a rapid decrease in the energy range $k^2=0.85$ to 1.6, followed by a slower fall off at higher energies. The rapid decrease above $k^2=1.0$ is due to rapidly diminishing contributions in the ^1D and ^1S partial waves. Qualitatively, the present results resemble those of the early pseudostate calculation of Burke and Webb,[3] in that they also reported a rapid decrease of cross section in the same energy range, but there are quantitative differences: The decrease in the range up to $k^2=1.6$ is less rapid than given in Ref. 3, and our cross section at higher energies is not flat but shows a continued decrease. Presumably the differences are due to the different pseudostate bases employed: the present is substantially larger (for $L\leq 3$) and is presumably more complete.

This cross section is sensitive to some extent to the method of amplitude-fitting employed. From comparison of results obtained with different orders of polynomials

TABLE IV. Amplitude for $2s$ excitation at selected energies.

	1.10		1.21		1.44		2.25		4.00	
k^2	R	I	R	I	R	I	R	I	R	I
^1S	0.100	0.150	0.142	0.107	0.128	0.056	0.091	−0.070	0.018	−0.094
^3S	−0.018	0.030	−0.008	0.037	0.013	0.040	0.045	0.007	0.037	−0.040
^1P	−0.002	−0.067	−0.018	−0.082	−0.022	−0.082	−0.056	−0.080	−0.075	−0.069
^3P	0.038	−0.050	0.030	−0.060	0.015	−0.058	−0.010	−0.062	−0.029	−0.061
^1D	0.066	0.023	0.061	0.015	0.033	0.006	−0.014	−0.015	−0.049	−0.026
^3D	−0.019	−0.027	−0.023	−0.030	−0.026	−0.031	−0.040	−0.032	−0.045	−0.034
^1F	0.024	−0.032	0.027	−0.035	0.025	−0.032	0.005	−0.027	−0.021	−0.018
^3F	0.015	0.001	0.012	−0.001	−0.004	−0.001	−0.017	−0.009	−0.032	−0.014
^1G	0.010	−0.019	0.015	−0.022	0.020	−0.022	0.014	−0.020	−0.005	−0.012
^3G	0.012	−0.012	0.014	−0.013	0.016	−0.011	0.003	−0.010	−0.014	−0.008
^1H	0.004	−0.008	0.007	−0.012	0.011	−0.015	0.010	−0.015	0.000	−0.012
^3H	0.004	−0.007	0.007	−0.010	0.010	−0.011	0.007	−0.010	−0.006	−0.008

TABLE V. Amplitude for $2p$ excitation at selected energies. The + or − indicates that the angular momentum of the scattered wave is $L\pm1$.

	1.10		1.21		1.44		2.25		4.00	
k^2	R	I	R	I	R	I	R	I	R	I
^1S	0.110	−0.110	0.086	−0.145	0.023	−0.164	−0.045	−0.146	−0.072	−0.096
^3S	0.038	0.014	0.049	0.002	0.058	−0.022	0.042	−0.072	−0.001	−0.084
$^1P_-$	0.025	−0.117	−0.003	−0.129	−0.022	−0.111	−0.054	−0.069	−0.047	−0.039
$^1P_+$	−0.070	0.000	−0.072	0.007	−0.080	0.000	−0.061	0.004	−0.050	−0.007
$^3P_-$	−0.024	−0.007	−0.020	−0.001	−0.006	−0.002	0.001	−0.013	−0.005	−0.022
$^3P_+$	−0.013	−0.042	−0.019	−0.044	−0.023	−0.038	−0.032	−0.034	−0.032	−0.026
$^1D_-$	−0.078	−0.138	−0.115	−0.136	−0.110	−0.113	−0.119	−0.063	−0.092	−0.037
$^1D_+$	0.034	−0.009	0.041	0.012	0.010	0.021	0.007	0.005	0.000	0.007
$^3D_-$	0.001	−0.037	−0.003	−0.042	−0.010	−0.049	−0.031	−0.051	−0.040	−0.042
$^3D_+$	−0.023	0.004	−0.025	0.004	−0.022	0.004	−0.026	0.005	−0.017	0.001
$^1F_-$	−0.067	−0.023	−0.084	−0.021	−0.091	−0.021	−0.122	−0.011	−0.101	−0.010
$^1F_+$	0.004	−0.014	0.007	−0.012	0.011	−0.011	0.014	−0.010	0.019	0.002
$^3F_-$	−0.041	−0.059	−0.047	−0.061	−0.058	−0.061	−0.074	−0.049	−0.067	−0.036
$^3F_+$	0.006	0.004	0.005	0.006	0.002	0.011	−0.002	0.009	0.000	0.008
$^1G_-$	−0.043	−0.009	−0.054	−0.010	−0.074	−0.008	−0.110	−0.008	−0.109	−0.013
$^1G_+$	0.002	−0.007	0.006	−0.008	0.009	−0.004	0.013	−0.007	0.021	0.002
$^3G_-$	−0.039	−0.017	−0.048	−0.019	−0.065	−0.021	−0.089	−0.025	−0.087	−0.023
$^3G_+$	0.005	−0.004	0.007	−0.001	0.006	0.002	0.006	0.004	0.009	0.007
$^1H_-$	−0.023	−0.004	−0.033	−0.004	−0.050	−0.005	−0.085	−0.004	−0.098	−0.006
$^1H_+$	0.001	−0.002	0.003	−0.004	0.006	−0.004	0.010	−0.003	0.019	−0.002
$^3H_-$	−0.023	−0.005	−0.032	−0.006	−0.048	−0.009	−0.077	−0.011	−0.086	−0.013
$^3H_+$	0.001	−0.002	0.004	−0.003	0.006	−0.001	0.008	0.001	0.013	0.003

and different ranges of energies included in the fit, I estimate that there is a residual uncertainty of about 10% in the $2s$-excitation cross section in the neighborhood of $k^2=1.0$ from this cause.

The $2p$ excitation cross section is reduced by a factor of about 1.9 compared to three-state close-coupling at 20 eV; the latter is only slightly less of an overestimate than in the case of the $2s$. The agreement between the present results and those of Burke and Webb,[3] although not outstanding, is better than was obtained for $2s$ excitation. In the present calculation, the maximum of the $2p$ cross section occurs at a somewhat higher energy ($k^2=3.0$ as compared to 2.25), but is about the same size ($\sim 0.87\pi a_0^2$) in comparison with the results of Ref. 2. This cross section is also sensitive to the amplitude-fitting technique. In this case, I have applied the fitting procedure separately to the low ($\sim k^2=1$) energy and the higher-energy ($k^2>2$) pseudoresonances. I estimate that the uncertainty in this cross section due to the fitting procedure to be also about 10% near $k^2=1.0$.

In order to investigate the extent to which the present results might depend on the pseudostate basis employed, I have calculated the contributions from $L\leq 3$ to elastic scattering and $n=2$ excitation for the single energy of $k^2=4.0$ for two additional pseudostate bases. These are the "variant 5-4-2" and the very tight pseudostates (VTPS) sets listed in Table I. The VTPS set, in particular, emphasizes short-range correlations and gave the best result for the $2s$ excitation cross section of those examined in Ref. 9 (however, those tests involved a highly restricted model). The incident energy of 4.0 Ry is a good one for these tests in that none of the sets investigated have a pseudothreshold close to that energy. Results are given in Table VI. The differences are not large, about 4% in the case of the $2s$ excitation, and less than 2% for the $2p$. It cannot be guaranteed that agreement is equally good at all energies, but the results certainly encourage belief in a reasonable level of adequacy of the set on which most of

TABLE VI. Sum of contributions from partial waves with $L\leq 3$ for $2s$ and $2p$ excitation at $k^2=4.0$ for the three psuedostate sets whose parameters are listed in Table I (units πa_0^2).

	$1s-2s$	$1s-2p$
Standard 5-4-2 basic set	0.0459	0.0932
Variant 5-4-2 basic set	0.0476	0.0923
VTPS	0.0477	0.0918

TABLE VII. Fitting coefficients for the collision strength [see Eq. (3.1)].

	Constrained		Unconstrained	
n_t	6	6	6	6
i	$2s$	$2p$	$2s$	$2p$
1	0.887 89	0.894 87	0.969 99	−21.110 29
2	−2.072 16	−11.943 40	−3.087 12	73.147 33
3	−0.561 83	23.771 62	4.126 30	−177.226 2
4	11.740 03	−25.047 69	1.573 42	275.520 9
5	−17.630 91	24.233 67	−7.205 37	−216.773 7
6	8.078 49	−12.000 09	4.003 58	66.952 48
7	0.0	4.439 43	0.0	11.263 24

the present calculations are based. At the other end of the energy range, the present results for $2s$ and $2p$ excitation at $k^2=0.91$ agree to better than 0.5% with results based on an 18-state expansion.

I have summarized the results for the convenience of potential users of this data by presenting (Table VII) least-squares fits to the collision strength, Ω ($\Omega=2k^2\sigma$). I write

$$\Omega(x)=\sum_{i=1}^{n_t} a_i/x^{i-1}+a_{n_t+1}\ln x \tag{3.1}$$

in which $x=k^2/E_x$, E_x being the excitation energy (0.75 Ry in the present case). These forms are suggested by the Born approximation, and enable simple evaluation of contributions to excitation rate coefficients. The coefficients obtained in a least-squares fit are given in Table VII.

The fits are of two types. In the type labeled "constrained" the coefficients a_1 and a_{n_t+1} have been fixed at the values determined from the first Born approximation. This means that the fits, if used as an extrapolation at energies higher than those for which calculations are reported here, will approach the results of the first Born approximation smoothly as energy increases. The accuracy of these is better than 3% at all points for both the $2s$ and the $2p$ states. The unconstrained fits do not have any restriction and are therefore slightly more accurate as fits to the actually calculated cross sections in the range considered, but should not be used for extrapolation to higher energies.

It is possible to compare the present result with those of other groups at $k^2=4.0$. A particularly interesting comparison is with the work of Bransden, McCarthy, Mitroy, and Stelbovics[16] (hereafter BMMS). These authors have studied electron-hydrogen scattering at 54.4 and 200 eV in several calculations, of which we are concerned with two: a coupled-channels optical potential calculation (CCO), and a pseudostate calculation containing the exact $1s$, $2s$, and $2p$ states plus seven pseudostates (4 s and 3 p). Numerical results are presented in Table VIII. The agreement between our results and their pseudostate calculation for elastic scattering and $2p$ excitation is rather good, but we have obtained a $2s$ excitation cross section about 20% larger than theirs. The agreement with their optical potential calculation is not good either for elastic scattering or for $2s$ excitation. Possibly, 54.4 eV may be too low an energy for successful use of their CCO method.

TABLE VIII. Cross sections (units πa_0^2) at $k^2=4$. References BMS, Ref. 15; BW, Ref. 2; EMM, Ref. 4; Morgan, Ref. 3; three-state close coupling (3CC), Ref. 14; Expt., Ref. 16.

	Elastic	$1s-2s$	$1s-2p$
Present	0.920	0.066	0.849
BMMS (CCO)	1.035	0.080	0.875
BMMS (PP)	0.926	0.053	0.856
BW		0.065	0.800
EMM (LE)		0.094	0.883
Morgan		0.063	0.814
3CC		0.101	0.908
Expt.			0.89±0.08

TABLE IX. Cross sections (units πa_0^2) at $k^2=2.58$. EMM, Ref. 4; Morgan, Ref. 3.

	Elastic	$1s-2s$	$1s-2p$
Present ($k^2=2.58$)	1.643	0.082	0.862
EMM (LE)		0.126	1.010
Morgan		0.097	0.828

I also quote in Table VIII results of Burke and Webb (BW, Ref. 3), Edmonds, McDowell, and Morgan (EMM, Ref. 5), and Morgan (Ref. 4). The calculation of Burke and Webb has been discussed previously. Their $2s$ excitation cross section agrees well with ours at this energy whereas the $2p$ excitation seems somewhat low. The close-coupling calculations of EMM quoted here incorporate of the $n=1$, 2, 3, and 4 states with exchange inlcuded in a local approximation only. The calculations of Morgan involve a 13-state basis (6 s, 5 p, 2 d) but neglect exchange. At this energy, the neglect of exchange does not lead to a large difference with respect to the present results. Three-state close-coupling (with exchange) results according to Ref. 16 are also included.

The unsatisfactory nature of the available experimental information at this and other energies above the $n=3$ threshold is discussed in Ref. 1. There is for the $2p$ excitation an absolute measurement due to Williams.[17] Almost all of the theoretical values presented in Table VIII agree with this result within the estimated experimental uncertainty (approximately 9%). It is to be regretted that there is no absolute measurement of the $2s$ excitation in this energy range. A previous estimate[1] involving renormalization of graphically presented experimental data of Kauppila *et al.*[18] and a correction for cascade from higher p states gives $\sigma_{1s\to 2s}\approx 0.060\pi a_0^2$ at $k^2=4.0$ in moderately satisfactory agreement with the present results and some of the other calculations quoted. But the situation is very uncertain. As for elastic scattering, only measurements of differential cross sections exist at the energies of interest here.[19,20] Our previous calculations are generally in good agreement with these.[20]

In Table IX, I compare the present values with the pseudostate calculations of Morgan and the $n=4$ close-coupling (local exchange) calculations of Edmonds *et al.* at 35 eV. Evidently neglect of continuum contributions and inaccurate treatment or neglect of exchange have a serious effect at this energy, particularly on the $2s$ excitation.

IV. EFFECTIVE COLLISION STRENGTHS

The results described in the previous section can be combined with the cross sections I have calculated previously between the $n=2$ and 3 thresholds to give a reasonably comprehensive representation of $n=2$ excitation from threshold through the intermediate energy range. These results are sufficient to enable calculation of rate coefficients or equivalent quantities for astrophysical and laboratory plasmas. The quantity presented here is the effective collision strength γ defined by

$$\gamma=\frac{1}{kT}\int_0^\infty e^{-E_f/kT}\Omega(E_f)dE_f \tag{4.1}$$

in which E_f is the energy of the incident electron measured with respect to the excited state, T is the plasma electron temperature, and k is Boltzmann's constant.

The conventional rate coefficient q is related to γ by[21]

$$q=\frac{8.63\times10^{-6}\gamma e^{-E_x/kT}}{\sqrt{T}g_i}\ \mathrm{cm^3\,sec^{-1}} \tag{4.2}$$

in which E_x is the excitation energy, the temperature T is in degrees, and g_i is the degeneracy of the initial state. (The convention is that $g_i=2$ for the hydrogen $1s$ state.) The effective collision strength is, however, more suitable for presentation here than q because it is dimensionless, and because it is a much slowly varying function of temperature at low temperatures.

I have calculated γ for $2s$ and $2p$ excitations using the Born constrained fits [Eq. (3.1)] for $k^2>0.90$ ($E_f>0.15$). Below $k^2=0.90$, I use the empirical representation given in Ref. 1. For the cross sections from $k^2=0.75$ to 0.85 a.u., I use

$$\sigma_{1s-2s}/\pi a_0^2=1.3\times10^{-4}\delta(E-E_{\mathrm{sr}})+0.13+0.89(E-0.75\mathrm{Ry})\ , \tag{4.3}$$

$$\sigma_{1s-2p}/\pi a_0^2=1.6\times10^{-3}\delta(E-E_{\mathrm{sr}})+0.16+2.0(E-0.75\mathrm{Ry})\ . \tag{4.4}$$

The delta function represents the contribution of the shape resonance close to threshold ($E_{\mathrm{sr}}=0.7512$ Ry). From $k^2=0.85$ to 0.90 a.u., I use

$$\sigma_{1s-2s}/\pi a_0^2=0.204\ ,\quad \sigma_{1s-2p}/\pi a_0^2=0.367\ , \tag{4.5}$$

which are averages of the (numerical) cross sections calculated in the resonance region in Ref. 2. Use of these formulas enables the analytic evaluation of the integral in Eq. (4.1).

The resulting effective collision strengths are given in Table X. They seem to be somewhat smaller (by about 10—20%) than those deduced from the recent work of Aggarwal[22] in the temperature range 15 000—50 000 K.

TABLE X. Effective collision strengths.

kT (Ry)	γ_{2s}	γ_{2p}
0.05	0.252	0.400
0.10	0.265	0.462
0.15	0.274	0.562
0.20	0.281	0.673
0.25	0.287	0.787
0.30	0.292	0.903
0.35	0.297	1.020
0.40	0.301	1.136
0.45	0.306	1.251
0.50	0.310	1.365
0.60	0.318	1.589
0.70	0.326	1.807
0.80	0.334	2.018
0.90	0.342	2.222
1.00	0.350	2.418

This probably results from the differences between the present calculation and those available to Aggarwal close to the ionization threshold. The agreement with Aggarwal's result is much better at low temperatures (5000 K) and at high temperatures (100 000 K).

V. CONCLUSION

I have reported here results of 11-state calculations of integrated cross sections for elastic scattering and $n=2$ excitation in electron-hydrogen interactions through the range from 12.2 to 54 eV. Pseudoresonances and pseudothreshold structure produced by our basis set have been removed by an amplitude-fitting procedure. The present results have been compared with other recent calculations and to the very limited extent possible, with experiment. The greatest remaining uncertainties in the cross section discussed in this work are probably in the range from the $n=3$ threshold to about 25 eV incident energy. I hope that the presentation of these computations will serve as a stimulus and a challenge to experiment to tell us what is really happening in this range.

[1] J. Callaway and M. R. C. McDowell, Comments At. Mol. Phys. **13**, 19 (1983).
[2] J. Callaway, Phys. Rev. A **26**, 199 (1982).
[3] P. G. Burke and T. G. Webb, J. Phys. B **3**, L131 (1970).
[4] L. A. Morgan, J. Phys. B **15**, 4247 (1982).
[5] P. W. Edmunds, M. R. C. McDowell, and L. A. Morgan, J. Phys. B **16**, 2553 (1983).
[6] J. Callaway, Phys. Rep. **45**, 89 (1978).
[7] J. Callaway, Phys. Letts. **100A**, 415 (1984).
[8] P. G. Burke, K. A. Berrington, and C. V. Sukumar, J. Phys. B **14**, 289 (1981).
[9] D. H. Oza and J. Callaway, Phys. Rev. A **27**, 2840 (1983).
[10] D. H. Oza, Phys. Rev. A **30**, 1101 (1984).
[11] N. Abu-Salbi and J. Callaway, Phys. Rev. A **24**, 2372 (1981).
[12] R. L. Armstead, Phys. Rev. **171**, 91 (1968).
[13] J. P. Lyons and R. K. Nesbet, J. Comput. Phys. **4**, 499 (1969).
[14] W. C. Fon, K. A. Berrington, P. G. Burke, and A. E. Kingston, J. Phys. B **14**, 1041 (1981).
[15] A. E. Kingston, W. C. Fon, and P. G. Burke, J. Phys. B **9**, 605 (1976).
[16] B. H. Bransden, I. E. McCarthy, J. D. Mitroy, and A. T. Stelbovics (unpublished).
[17] J. F. Williams, J. Phys. B **14**, 1197 (1981).
[18] W. E. Kauppila, W. R. Ott, and W. L. Fite, Phys. Rev. A **1**, 1099 (1970).
[19] J. F. Williams, J. Phys. B **8**, 2191 (1975).
[20] J. Callaway and J. F. Williams, Phys. Rev. A **12**, 2312 (1975).
[21] S. S. Tayal and A. E. Kingston, J. Phys. B **17**, 1383 (1984).
[22] K. M. Aggarwal Mon. Not. R. Astron. Soc. **202**, 15P (1983).